

Nucleophilic Substitution at the Imidoyl Carbon Atom: Intermediate Mechanistic and Reactivity Behavior between Carbonyl and Vinyl Carbon Substitution

Hong Guang Li, Chang Kon Kim, Bon-Su Lee, Chan Kyung Kim, Soon Ki Rhee,[†] and Ikchoon Lee*

Contribution from the Department of Chemistry, Inha University, Incheon, 402-751, Korea, and Department of Chemistry, Chonnam National University, Kwangju, 500-757, Korea

Received September 12, 2000. Revised Manuscript Received December 26, 2000

Abstract: Gas-phase nucleophilic substitution reactions at the imidoyl carbon have been investigated using chloride exchanges, $\text{Cl}^- + \text{RY}=\text{CHCl} \rightleftharpoons \text{RY}=\text{CHCl} + \text{Cl}^-$ with $\text{Y} = \text{N}$ and $\text{R} = \text{F}, \text{H}$ or CH_3 , at the MP2, B3LYP and G2(+) levels using the MP2/6-311+G** geometries. The results are compared with those for the vinyl ($\text{Y} = \text{CH}$) and carbonyl ($\text{Y} = \text{O}$) carbon substitution. The mechanism and reactivity of substitution at the imidoyl carbon are intermediate between those of carbonyl ($\text{S}_{\text{N}}\pi$) and vinyl carbon ($\text{S}_{\text{N}}\sigma$) substitution, which is directly related to the electronegativity of Y , $\text{CH} < \text{N} < \text{O}$. The prediction of competitive $\text{S}_{\text{N}}\sigma$ with $\text{S}_{\text{N}}\pi$ path for the imidoyl chloride is consistent with the $\text{S}_{\text{N}}1$ -like mechanism proposed for reactions in solution. The important factors in favor of an in-plane concerted $\text{S}_{\text{N}}2$ ($\text{S}_{\text{N}}\sigma$) over an out-of-plane π -attack ($\text{S}_{\text{N}}\pi$) path are (i) lower proximate $\sigma-\sigma^*$ charge-transfer energies (ΔE_{CT}), (ii) stronger electrostatic stabilization (ΔE_{NCT}), and (iii) larger lobe size on C_α for the σ^* - than π^* -LUMO despite the higher σ^* than π^* level. The electron correlation energy effects at the MP2 level are overestimated for the relatively delocalized structure ($\text{S}_{\text{N}}\pi$ TS) but are underestimated for the localized structure ($\text{S}_{\text{N}}\sigma$ TS) so that the MP2 energies lead to a wrong prediction of preferred reaction path for the vinyl chloride. The DFT at the B3LYP level predicts correct reaction pathways but overestimates the electron correlation effects.

Introduction

Nucleophilic substitution reactions at vinylic carbon have been shown to proceed through a range of different reaction pathways with a broad spectrum of reaction mechanisms.¹ In most vinylic substitution reactions, the nucleophile approaches the vinylic carbon perpendicularly and leads normally to a retention product through a tetrahedral intermediate ($\text{Ad}_{\text{N}}-\text{E}$ mechanism),² although partial or complete stereoconvergence may result when the intermediate has a long lifetime.^{1a-e} However, recently possibility of the vinylic substitution proceeding through an in-plane $\text{S}_{\text{N}}2$ route with inversion of configuration has been shown theoretically³ as well as experimentally in solution.^{2,4} This in-plane concerted $\text{S}_{\text{N}}2$ reaction at vinylic carbon ($\text{S}_{\text{N}}2\text{-Vin}$ or $\text{S}_{\text{N}}\sigma$ path) is more likely to be found in the reaction with a weak nucleophile (e.g., Cl^- , Br^- , etc.) coupled with a strong nucleo-

fuge (e.g., Cl^- , PhI , triflate, etc.) proceeding through a loose $\text{S}_{\text{N}}1$ -like transition state (TS).^{3,4} Experimentally in the gas phase the $\text{S}_{\text{N}}\sigma$ reactivity of chloride exchange in vinyl chloride has been shown to be too slow to be observed, but for exothermic reactions of greater reactivity such pathway, $\text{S}_{\text{N}}\sigma$, is predicted to be feasible.^{4g}

In contrast, the gas-phase nucleophilic substitution reactions at carbonyl carbon are found to proceed exclusively through an out-of-plane π -attack mechanism ($\text{S}_{\text{N}}\pi$ path)⁵ with relatively tight TS, for example, for the chloride exchanges in formyl and acetyl chlorides the bond formation has progressed to ~61%, whereas the C–Cl bond cleavage has occurred only to 39%, in the TS.⁵ Our high level ab initio studies revealed that for the gas-phase chloride exchange reactions of formyl and acetyl chlorides, the $\text{S}_{\text{N}}\sigma$ pathway is not only unfeasible (since the σ -adducts of C_{2v} symmetry, either as a TS or a stable intermediate, cannot be located) but also constituted a much higher barrier path than the $\text{S}_{\text{N}}\pi$ path.⁵

Since the ethenes and carbonyl compounds are structurally related but differ mechanistically for the nucleophilic substitu-

* Author to whom correspondence should be addressed. Fax: +82-32-865-4855. E-mail: ilee@inha.ac.kr.

[†] Chonnam National University.

(1) (a) Rappoport, Z. *Adv. Phys. Org. Chem.* **1969**, 7, 1. (b) Rappoport, Z. *Acc. Chem. Res.* **1981**, 14, 7. (c) Modena, G. *Acc. Chem. Res.* **1971**, 4, 73. (d) Miller, S. I. *Tetrahedron*, **1977**, 33, 1211. (e) Stang, P. J.; Rappoport, Z.; Hanack, M.; Subramanian, L. R. *Vinyl Cations*; Academic Press: New York **1979**. (f) Shainyan, B. A.; Rappoport, Z. *J. Org. Chem.* **1993**, 58, 342. (g) Galli, C.; Gentili, P.; Rappoport, Z. *J. Org. Chem.* **1994**, 59, 6786. (h) Bernasconi, C. F.; Schuck, D. F.; Ketner, R. J.; Wess, M.; Rappoport, Z. *J. Am. Chem. Soc.* **1994**, 116, 11764. (i) Beit-Yannai, M.; Rappoport, Z.; Shainyan, B. A.; Danilevich, Y. S. *J. Org. Chem.* **1997**, 62, 8049. (j) Chen, X.; Rappoport, Z. *J. Org. Chem.* **1998**, 63, 5684. (k) Rappoport, Z. *Acc. Chem. Res.* **1992**, 25, 474.

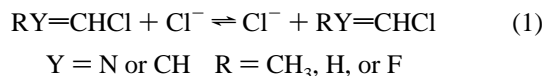
(2) Lucchini, V.; Modena, G.; Pasquato, L. *J. Am. Chem. Soc.* **1993**, 115, 4527.

(3) (a) Glukhovtsev, M. N.; Pross, A.; Radom, L. *J. Am. Chem. Soc.* **1994**, 116, 5961. (b) Kim, C. K.; Hyun, K. H.; Kim, C. K.; Lee, I. *J. Am. Chem. Soc.* **2000**, 122, 2294.

(4) (a) Clarke T. C.; Kelsey, D. R.; Bergman, R. G. *J. Am. Chem. Soc.* **1972**, 94, 3626. (b) Summerville, R. H.; Senkler, C. A.; Schleyer, P. v. R.; Dueber, T. E.; Stang, P. J. *J. Am. Chem. Soc.* **1974**, 96, 1100. (c) Lucchini, V.; Modena, G.; Valle, G.; Capozzi, G.; *J. Org. Chem.* **1981**, 46, 4720. (d) Ochiai, M.; Oshima, K.; Masaki, Y. *J. Am. Chem. Soc.* **1991**, 113, 7059. (e) Okuyama, T.; Ochiai, M. *J. Am. Chem. Soc.* **1997**, 119, 4785. (f) Okuyama, T.; Takino, T.; Sato, K.; Ochiai, M. *J. Am. Chem. Soc.* **1998**, 120, 2275. (g) Kennedy, R. A.; Mayhew, C. A.; Peverall, R.; Watts, P. *Phys. Chem. Chem. Phys.* **2000**, 2, 3245.

(5) (a) Lee, I.; Lee, D.; Kim, C. K. *J. Phys. Chem. A* **1997**, 101, 879. (b) Kim, C. K.; Li, H. G.; Sohn, C. K.; Chun, Y. I.; Lee, I. *J. Phys. Chem. A* **2000**, 104, 4069. (c) Lee, I.; Kim, C. K.; Li, H. G.; Sohn, C. K.; Kim, C. K.; Lee, H. W.; Lee, B.-S. *J. Am. Chem. Soc.* **2000**, 122, 11162.

tion, it would be of much interest to investigate the nucleophilic substitution mechanism of another structurally similar compounds that are likely to show intermediate behavior. In this work, we extend our studies to the nucleophilic substitution at the methine carbon atom, eq 1 with $Y = N$ and $R = CH_3, H,$ or F , and aim to elucidate the mechanism, in particular to examine various factors causing the energetic preference for the in-plane σ -attack ($S_N\sigma$ route) over the out-of-plane π -attack ($S_N\pi$ route) by comparing the MO theoretical results for the three chloride exchange reactions of vinyl ($Y = CH$), imidoyl ($Y = N$) and carbonyl ($Y = O$; for this there is no R) chlorides.



The imidoyl chlorides (also called as imidyl or imino chlorides) can be considered to be derivatives of the hypothetical imidic acid, $R(OH)C=NH$, in which the hydroxyl group has been replaced by a chlorine.

For comparison, we have also performed similar calculations on the chloride exchanges of vinyl chlorides ($Y = CH$, with $R = CH_3, H,$ or F) at the same theoretical level, that is, $G2(+)//MP2/6-311+G^{**}$.

Calculations

Calculations were carried out using the *Gaussian 98* set of programs.⁶ All geometries of the reactants and stationary-point structures were fully optimized at the $MP2/6-311+G^{**}$ level throughout in this study. For comparison, geometries were also optimized at the $QCISD$ and $B3LYP$ levels with the $6-311+G^{**}$ basis set. The stationary points were characterized by harmonic vibrational analysis employing energy Hessians at two levels: $MP2/6-311+G^{**}$ and $B3LYP/6-311+G^{**}$. The TSs were confirmed to be located on the reaction path from the reactants to the product for both $Y = NH$ and CH_2 by performing intrinsic reaction coordinate calculations at the $MP2$ level.^{7a} For the reactions of $HN=CHCl$ and $CH_2=CHCl$ with Cl^- , activation energies (ΔE^\ddagger values) were evaluated also at the $G2(+)$ $MP2$, $G2(+)$ and $QCISD(T)/6-311+G(3df,2p)$ levels.^{7b} The activation energies (ΔE^\ddagger) were corrected for zero-point vibrational energies (ZPE) with application of appropriate scaling factors⁸ and thermal energies (ΔH^\ddagger), and applied entropies to obtain free energy changes (ΔG^\ddagger) at 298 K. Energetics for all the reactions studied, eq 1, were discussed on the basis of those at the $G2(+)$ level.^{7b} All of the activation energies (ΔE^\ddagger , ΔH^\ddagger , and ΔG^\ddagger) reported are relative to the separated reactants level. The natural bond orbital (NBO) analyses⁹ were performed to determine the proximate $\sigma-\sigma^*$ (which includes $n-\sigma^*$, $n-\pi^*$, $\sigma-\pi^*$, etc.) charge-transfer energies in the substrates and transition states (TSs), and natural population

(6) Frisch, M. J.; Trucks, G. W.; Schlegel, H. B.; Scuseria, G. E.; Robb, M. A.; Cheeseman, J. R.; Zakrzewski, V. G.; Montgomery, J. A., Jr.; Stratmann, R. E.; Burant, J. C.; Dapprich, S.; Millam, J. M.; Daniels, A. D.; Kudin, K. N.; Strain, M. C.; Farkas, O.; Tomasi, J.; Barone, V.; Cossi, M.; Cammi, R.; Mennucci, B.; Pomelli, C.; Adamo, C.; Clifford, S.; Ochterski, J.; Petersson, G. A.; Ayala, P. Y.; Cui, Q.; Morokuma, K.; Malick, D. K.; Rabuck, A. D.; Raghavachari, K.; Foresman, J. B.; Cioslowski, J.; Ortiz, J. V.; Stefanov, B. B.; Liu, G.; Liashenko, A.; Piskorz, P.; Komaromi, I.; Gomperts, R.; Martin, R. L.; Fox, D. J.; Keith, T.; Al-Laham, M. A.; Peng, C. Y.; Nanayakkara, A.; Gonzalez, C.; Challacombe, M.; Gill, P. M. W.; Johnson, B.; Chen, W.; Wong, M. W.; Andres, J. L.; Gonzalez, C.; Head-Gordon, M.; Replogle, E. S.; Pople, J. A. *Gaussian 98*, revision A.6.; Gaussian, Inc.: Pittsburgh, PA, 1998.

(7) (a) Foresman, J. B.; Frisch, A. E. *Exploring Chemistry with Electronic Structure Methods*, 2nd ed.; Gaussian, Inc.: Pittsburgh, 1996; Chapter 8. (b) Reference 7a, Chapter 7.

(8) Scott, A. P.; Radom, L. *J. Phys. Chem.* **1996**, *100*, 16502.

(9) (a) Reed, A. E.; Curtiss, L. A.; Weinhold, F. *Chem. Rev.* **1988**, *88*, 899. (b) Glendening, E. D.; Weinhold, F. *J. Comput. Chem.* **1998**, *19*, 593 and 610. (c) Glendening, E. D.; Badenhop, J. K.; Weinhold, F. *J. Comput. Chem.* **1998**, *19*, 628.

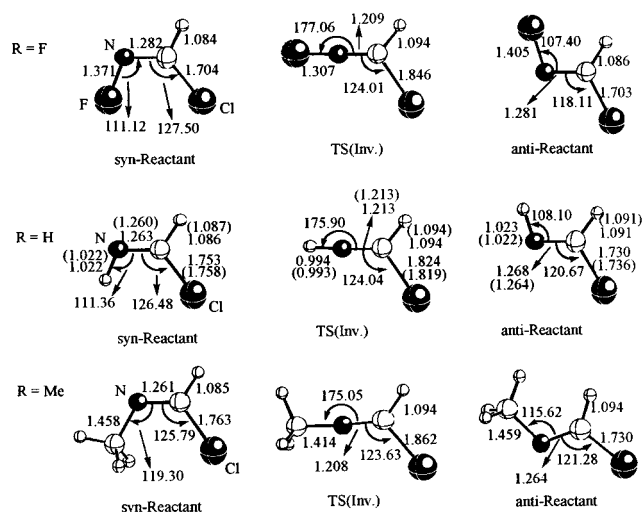
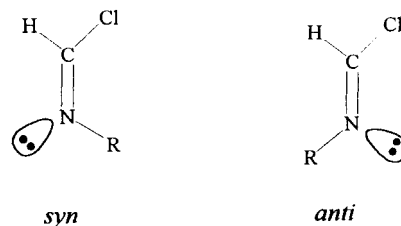


Figure 1. Structures of reactants and inversion transition states, at the $MP2/6-311+G^{**}$ for $Y = N$ (bond lengths in Å, and angles in degrees). Values in parenthesis are at the $QCISD/6-311+G^{**}$ level.

analyses (NPA)^{9a} were carried out. For bond order analyses, the $PM3$ method¹⁰ was used.

Results and Discussion

(I) Reactants and Reactant Complexes (RC). In principle the imidoyl halides can exist in two possible configurations, which are *syn* and *anti* with respect to the N -substituent and the leaving group, chlorine atom.¹¹ For imidoyl chlorides with



aryl substituents (e.g., $p\text{-NO}_2\text{C}_6\text{H}_4\text{CCl}=\text{NC}_6\text{H}_4\text{NO}_2$) dipole moment measurements suggested that the *syn*-configuration predominates.¹² In the present work, for all R 's ($R = CH_3, H,$ and F) the *syn* forms are found to be more stable than the *anti* forms by $\sim 1\text{--}2$ kcal mol^{-1} (Table S1, Supporting Information) at the $G2(+)$ level. This trend is easily explained by the relatively strong vicinal antiperiplanar $n_N-\sigma^*_{C-Cl}$ charge-transfer interaction in the *syn* forms.^{9,13} Indeed, the geometries in Figure 1 show that bond length of $C=N$ is shorter (by ~ 0.005 Å for $R = H$) and that of $C-Cl$ is longer (by ~ 0.023 Å for $R = H$) in the *syn* form than in the *anti* form as required by a stronger vicinal $n-\sigma^*$ charge-transfer interaction in the *syn* (antiperiplanar configuration) than in the *anti* form (synperiplanar configuration). For $R = F$, there is a weak opposing vicinal $\sigma-\sigma^*$ interaction involving a strong polar $N-F$ bond, for example,

(10) Stewart, J. J. P. *J. Comput. Chem.* **1989**, *10*, 209 and 221; Stewart, J. J. P. *J. Comput. Chem.* **1990**, *11*, 543; Stewart, J. J. P. *J. Comput. Chem.* **1991**, *12*, 320.

(11) Bonnett, R. In *The Chemistry of the Carbon-Nitrogen Double Bond*; Patai, S., Ed.; Interscience: New York, 1970; Chapter 13.

(12) Greenberg, B.; Aston, J. G. *J. Org. Chem.* **1960**, *25*, 1894.

(13) (a) Epiotis, N. D.; Cherry, W. R.; Shaik, S.; Yates, R. L.; Bernardi, F. *Structural Theory of Organic Chemistry*; Springer-Verlag: Berlin, 1977; Chapter IV. (b) Brunck, T. K.; Weinhold, F. *J. Am. Chem. Soc.* **1979**, *101*, 1700. (c) Musso, G. F.; Figari, G.; Magnasco, V. *J. Chem. Soc., Faraday Trans. 2* **1985**, *81*, 1243. (d) Tyrell, J.; Weinstock, R. B.; Weinhold, F. *Int. J. Quantum Chem.* **1981**, *19*, 781. (e) Reed, A. E.; Weinhold, F. *J. Am. Chem. Soc.* **1986**, *108*, 3586.

Table 1. Calculated Gas-Phase Activation Energies at Various Levels of Theory for the Two S_N Paths, $S_N\pi$ and $S_N\sigma$, with $Y = N$ and CH (in kcal mol⁻¹)

Y	levels of theory	$\Delta E^\ddagger(\pi)^a$	$\Delta E^\ddagger(\sigma)^a$	$\delta\Delta E^\ddagger = \Delta E^\ddagger(\sigma) - \Delta E^\ddagger(\pi)$
N	MP2/6-311+G**	5.76	19.25	+13.49
	B3LYP/6-311+G**	4.38	9.78	+5.40
	QCISD/6-311+G**	10.64	19.06	+8.42
	G2(+)/MP2 ^b	6.88	14.88	+8.00
	G2(+) ^b	7.29	14.94	+7.65
	QCISD(T)/6-311+G(3df,2p) ^b	7.69	14.95	+7.26
CH	MP2/6-311+G**	26.80	29.22	+2.42
	B3LYP/6-311+G**	26.78	18.09	-8.69
	QCISD/6-311+G**	31.65	27.41	-4.24
	G2(+)/MP2 ^b	28.29	23.00	-5.29
	G2(+) ^b	28.78	23.39	-5.39
	QCISD(T)/6-311+G(3df,2p) ^b	29.29	23.88	-5.41

^a Not corrected for zero-point vibrational energy. ^b Using MP2/6-311+G** geometry.

$\sigma_{CH} - \sigma_{N-F}^*$ and $n_F - \pi_{C=N}^*$, so that there are little bond length changes. The barriers to inversion from syn to anti are relatively high (S1), for example, 21.6 kcal mol⁻¹ for $R = H$ at the G2-(+) level. This means that, although energy differences between the two configurations are small, the interconversion is difficult, and the syn form will be predominant in the room temperature. For the substituted ($R = F$ and CH_3) vinyl chlorides the energy differences between the syn and anti forms are much smaller (<1.0 kcal mol⁻¹ at the G2(+) level, S1) since in the vinyl chlorides only the weak $\sigma - \sigma^*$ type interactions are involved due to the lack of a lone pair orbital (n), that is, there is no strong $n - \sigma^*$ type^{9,13} interaction available in the syn, nor in the anti, form. The inversion occurs by migration of R at nitrogen within the molecular plane rather than by rotation about the carbon–nitrogen double bond with the TS corresponding to the $R-N=C$ linear arrangement (Figure 1).

The gas-phase nucleophilic substitutions of imidoyl chlorides with Cl^- proceed through double-well potential energy surfaces with TSs between the two identical ion–dipole complexes, reactant (RC) and product (PC) complexes, of electrostatic nature. Since the reactions are thermoneutral, the thermodynamic barriers are zero, and the central barriers from the reactant complexes to the transition states are intrinsic barriers, ΔE_o^\ddagger . For imidoyl chloride reacting via $S_N\sigma$ path the RC and PC turned out to be different so that the central barrier is not an intrinsic barrier. The structures and energies of the reactant complexes are summarized in Table S2 (Supporting Information).

(II) Nucleophilic Substitution Reactions. To examine the relative accuracies of a variety of different method and levels of sophistication up to the QCISD(T)/6-311+G(3df,2p) level, the activation energies (relative to the separated reactants level) involved in both the $S_N\pi$ and $S_N\sigma$ paths for the chloride exchanges in imidoyl ($HN=CHCl$) and vinyl chlorides ($CH_2=CHCl$) are calculated using the MP2/6-311+G** optimized geometries as presented in Table 1. We note in this Table that only the MP2/6-311+G** level energies lead to a qualitatively wrong prediction of the preferred reaction path for the vinyl chloride ($\delta\Delta E^\ddagger = \Delta E^\ddagger(\sigma) - \Delta E^\ddagger(\pi) > 0$); the results at the MP2/6-311+G** level are poor both qualitatively and quantitatively. This is mainly because electron correlation energy effects are overestimated¹⁵ for the relatively delocalized form ($S_N\pi$ TS) and underestimated for the localized form ($S_N\sigma$ TS) at the MP2 level as the lower $\Delta E^\ddagger(\pi)$ and higher $\Delta E^\ddagger(\sigma)$ values than those corresponding values at the higher level of G2(+) shown in Table 1. Although the DFT method (at the B3LYP/6-311+G** level) predicts the preferred reaction paths correctly

Table 2. Energetics for the Gas-Phase Reactions $RY=CHCl + Cl^- \rightleftharpoons Cl^- + RY=CHCl$, Calculated at the MP2/6-311+G** Level with $Y = N$ and CH (in kcal mol⁻¹)

Y	R	path		ΔE^\ddagger^a	ΔH^\ddagger	$-T\Delta S^\ddagger$	ΔG^\ddagger	
F	inv. ^b	(TS) ^c		63.33	63.52	-0.54	63.0	
		(TS) ^c	syn	1.74	1.01	8.50	9.5	
		(TS) ^c	anti	7.88	7.06	8.36	15.4	
	$S_N\sigma$	(2f) ^d		30.45	29.88	7.86	37.7	
		(TS) ^c	inv. ^b	21.68	21.73	-0.16	21.6	
		(TS) ^c	syn	5.53	4.80	8.05	12.9	
N	inv. ^b	(TS) ^c	anti	12.96	12.18	8.15	20.3	
		(TS) ^c		16.66	16.82	5.17	22.0	
		(TS) ^c	syn	21.80	21.89	-0.74	21.2	
	$S_N\pi$	(TS) ^c	anti	4.08	3.49	8.10	11.6	
		(TS) ^c		14.55	13.81	8.06	21.9	
		(TS) ^c	syn	10.83	11.27	4.49	15.8	
Me	$S_N\sigma$	(TS) ^c	syn	25.69	25.18	7.89	33.1	
		(TS) ^c	anti	28.19	27.58	7.93	35.5	
		(TS) ^c		28.12	27.94	6.85	34.8	
	CH	$S_N\pi$	(TS) ^c		26.20	25.50	8.07	33.6
		(TS) ^c	syn	28.05	27.75	7.13	34.9	
		(TS) ^c	anti	26.69	26.18	7.77	34.0	
Me	$S_N\pi$	(TS) ^c		29.00	28.36	7.94	36.3	
	(TS) ^c	syn	29.43	29.20	7.08	36.3		

^a Corrected for zero-point vibrational energy (ZPE). ZPEs were scaled by the factor of 0.9748.⁸ ^b Internal inversion barrier of substrate from syn- to anti form. ^c Transition state, confirmed by only one negative eigenvalue in the Hessian matrix. ^d Two negative eigenvalues in the Hessian matrix.

in both cases ($Y = N$ and CH), the ΔE^\ddagger values are too low, that is, correlation effects are overestimated. In both cases of $Y = N$ and CH , the QCISD/6-311+G** method leads to the too high ΔE^\ddagger values. As the level of calculation is raised progressively from G2(+)/MP2 to G2(+) and to QCISD(T)/6-311+G(3df,2p), the activation barriers, both $\Delta E^\ddagger(\pi)$ and $\Delta E^\ddagger(\sigma)$, tend to be elevated successively, albeit the increments are very small, and as a result the barrier height difference, $\delta\Delta E^\ddagger = \Delta E^\ddagger(\sigma) - \Delta E^\ddagger(\pi)$, becomes less positive (for $Y = N$) or more negative (for $Y = CH$). This means that as the level of calculation is raised, the $S_N\sigma$ path becomes relatively more favorable than the $S_N\pi$ path. This observation must be related to the involvement of a greater degree of electron pairing in the loose $S_N\sigma$ TS than in the $S_N\pi$ TS so that progressively better account of electron correlation effects for paired electrons at the higher level calculation provides improved results. The electron correlation energies are greater for intrapair than interpair, and for interpair involving a lone pair than a bond pair.¹⁵

In the loose $S_N\sigma$ TS, the two Cl atoms have larger number of electron pairs than those in the tight $S_N\pi$ TS, and also the partial triple bond provides greater degree of electron pairing in the former than the partial single bond in the latter. The higher degree of electron pairing should involve stronger electron correlation effects which should be properly accounted for by a more sophisticated level of calculation.

The energetics for the gas-phase nucleophilic substitution reactions of the imidoyl ($Y = N$) and vinyl ($Y = CH$) chlorides calculated at three levels, MP2/6-311+G**, B3LYP/6-311+G**, and G2(+)/MP2/6-311+G**, are summarized in Tables 2, 3, and 4, respectively. Examination of these Tables reveals that: (i) In no case is a stable adduct (π - or σ -type) formed, and all of the adducts correspond to transition states (with the exception of the $S_N\sigma$ adduct for $Y = N$ with $R = F$, for which two

(14) Raghavachari, K.; Whiteside, R. A.; Pople, J. A.; Schleyer, P. v. R. *J. Am. Chem. Soc.* **1981**, *103*, 5649.

(15) (a) Carsky, P.; Urban, M. *Ab Initio Calculations. Methods and Applications in Chemistry*; Springer-Verlag: Berlin, 1980; p 79. (b) Wilson, S. *Electron Correlation in Molecules*; Oxford University Press: Oxford, 1984; p 56.

Table 3. Energetics for the Gas-Phase Reactions $\text{RY}=\text{CHCl} + \text{Cl}^- \rightleftharpoons \text{Cl}^- + \text{RY}=\text{CHCl}$, Calculated at the B3LYP/6-311+G** Level with Y = N and CH (in kcal mol⁻¹)

Y	R	path		$\Delta E^{\ddagger a}$	ΔH^{\ddagger}	$-T\Delta S^{\ddagger}$	ΔG^{\ddagger}	
F	inv. ^b	(TS) ^c		56.74	56.95	-0.56	56.4	
		$\text{S}_{\text{N}}\pi$	syn	(TS) ^c	0.80	0.18	8.22	8.4
	$\text{S}_{\text{N}}\sigma$	anti	(TS) ^c	5.50	4.80	8.06	12.9	
			(2i) ^d	18.84	18.40	7.45	25.9	
		syn	(TS) ^c	18.16	18.23	-0.16	18.1	
		anti	(TS) ^c	3.89	3.29	7.69	11.0	
N	inv. ^b	(TS) ^c		11.55	10.93	7.74	18.7	
		$\text{S}_{\text{N}}\pi$	syn	(TS) ^c	7.66	7.67	5.92	13.6
	$\text{S}_{\text{N}}\sigma$	anti	(TS) ^c	16.70	16.71	-0.28	16.4	
		syn	(TS) ^c	3.86	3.41	7.77	11.2	
		anti	(TS) ^c	14.40	13.87	7.51	21.4	
			(TS) ^c	5.42	5.65	5.69	11.3	
F	$\text{S}_{\text{N}}\pi$	syn	(TS) ^c	24.62	24.20	7.71	31.9	
		anti	(TS) ^c	25.88	25.38	7.66	33.0	
CH	$\text{S}_{\text{N}}\sigma$	(TS) ^c		18.29	18.11	7.04	25.2	
		$\text{S}_{\text{N}}\pi$		25.84	25.26	7.76	33.0	
	H	$\text{S}_{\text{N}}\sigma$	(TS) ^c		16.76	16.49	7.18	23.7
			$\text{S}_{\text{N}}\pi$	syn	(TS) ^c	27.34	27.03	6.88
	Me	$\text{S}_{\text{N}}\pi$	anti	(TS) ^c	29.20	28.68	7.66	36.3
			$\text{S}_{\text{N}}\sigma$		(TS) ^c	18.75	18.61	6.86

^a Corrected for zero-point vibrational energy (ZPE). ZPEs were scaled by the factor of 0.9806.⁸ ^b Internal inversion barrier of substrate from syn- to anti form. ^c Transition state, confirmed by only one negative eigenvalue in the Hessian matrix. ^d Two negative eigenvalues in the Hessian matrix.

Table 4. Energetics for the Gas-Phase Reactions $\text{RY}=\text{CHCl} + \text{Cl}^- \rightleftharpoons \text{Cl}^- + \text{RY}=\text{CHCl}$, Calculated at the G2(+)/MP2/6-311+G** Level with Y = N and CH (in kcal mol⁻¹)

Y	R	path		$\Delta E^{\ddagger a}$	ΔH^{\ddagger}	$-T\Delta S^{\ddagger}$	ΔG^{\ddagger}	
F	inv. ^b	(TS) ^c		62.24	62.43	-0.54	61.9	
		$\text{S}_{\text{N}}\pi$	syn	2.81	2.07	8.50	10.6	
	$\text{S}_{\text{N}}\sigma$	anti	(TS) ^c	7.74	6.92	8.36	15.3	
			(TS) ^c	26.60	26.02	7.86	33.9	
		syn	(TS) ^c	21.59	21.65	-0.16	21.5	
		anti	(TS) ^c	7.07	6.33	8.05	14.4	
N	inv. ^b	(TS) ^c		13.68	12.90	8.15	21.1	
		$\text{S}_{\text{N}}\pi$	syn	7.07	6.33	8.05	14.4	
	$\text{S}_{\text{N}}\sigma$	anti	(TS) ^c	12.35	12.51	5.17	17.7	
		syn	(TS) ^c	21.35	21.45	-0.74	20.7	
		anti	(TS) ^c	5.77	5.18	8.10	13.3	
			(TS) ^c	15.87	15.13	8.06	23.2	
F	$\text{S}_{\text{N}}\pi$	syn	(TS) ^c	8.80	9.25	4.49	13.7	
		anti	(TS) ^c	27.61	27.10	7.89	35.0	
CH	$\text{S}_{\text{N}}\sigma$	(TS) ^c		29.71	29.10	7.93	37.0	
		$\text{S}_{\text{N}}\pi$		23.40	23.22	6.85	30.1	
	H	$\text{S}_{\text{N}}\sigma$	(TS) ^c		28.18	27.48	8.07	35.6
			$\text{S}_{\text{N}}\pi$		22.22	21.92	7.13	29.1
	Me	$\text{S}_{\text{N}}\pi$	syn	(TS) ^c	28.88	28.38	7.77	36.2
			anti	(TS) ^c	31.16	30.52	7.94	38.5
	$\text{S}_{\text{N}}\sigma$		(TS) ^c	23.78	23.54	7.08	30.6	

^a Corrected for the zero-point vibrational energy calculated at the MP2/6-311+G** level. ZPEs were scaled by the factor of 0.9748.⁸ ^b Internal inversion barrier of substrate from syn- to anti form.

imaginary frequencies were obtained). This is consistent with relatively narrow energy gaps, $\Delta\epsilon = \epsilon_{\sigma^*} - \epsilon_{\pi^*}$, between π^* and σ^* orbitals. It has been shown that for the adduct to have a long lifetime as an intermediate $\Delta\epsilon$ should be large.⁵ (ii) The syn configurations lead to lower activation barriers for the $\text{S}_{\text{N}}\pi$ paths. This is consistent with the stronger $\text{n}_{\text{N}}-\sigma_{\text{C}-\text{Cl}}^*$ interaction at the antiperiplanar arrangement.¹³ (iii) The preferred paths predicted at the B3LYP level agree with those at the higher G2(+) level, but those at the MP2 level fail to predict the preferred $\text{S}_{\text{N}}\sigma$ path (in disagreement with the G2(+) level) for vinyl substitution with R = F, H, and CH₃. In this respect, the lower level correlated (MP2) energetics are qualitatively inferior to the B3LYP level DFT energetics. (iv) A donor substituent, R = CH₃, lowers the $\text{S}_{\text{N}}\sigma$ -path barrier, whereas an acceptor, R = F, depresses the $\text{S}_{\text{N}}\pi$ -path barrier. These trends are manifesta-

Table 5. Canonical LUMO Levels for the Reactants with Y = N and CH, Calculated at the RHF/6-311+G**//MP2/6-311+G** Level (in au)

Y	R	syn		
		ϵ_{π^*}	ϵ_{σ^*}	$\Delta\epsilon_{(\sigma^*-\pi^*)}$
O	H	0.0795	0.1965	0.1170
		0.1150	0.2140	0.0990
N	Me	0.1002	0.1924	0.0922
		0.1162	0.2125	0.0963
CH	H	0.2025	0.2295	0.0240
		0.2178	0.2288	0.0110

tions of a positively charged double-bond moiety formation in the $\text{S}_{\text{N}}\sigma$ which is stabilized by a donor, and a negatively charged double-bond moiety formation in the $\text{S}_{\text{N}}\pi$ path which is stabilized by an acceptor. As a result, for the *N*-methylimidoyl chloride (R = CH₃) the reaction via the $\text{S}_{\text{N}}\sigma$ path becomes equally possible with that via the $\text{S}_{\text{N}}\pi$ path (the ΔG^{\ddagger} values are 13.3 and 13.7 kcal mol⁻¹ for the $\text{S}_{\text{N}}\pi$ and $\text{S}_{\text{N}}\sigma$ path respectively at the G2(+) level).

The energy change (ΔE) in the interaction of two molecules can be expressed as a sum of three major terms, charge transfer (ΔE_{CT}), electrostatic (ΔE_{es}), and exclusion repulsion (ΔE_{ex}) energies.¹⁶ The latter two are often combined to a noncharge-transfer term (ΔE_{NCT}).^{9a} The charge-transfer energy (ΔE_{CT}) can be estimated by a second-order perturbation energy, $\Delta E_{\sigma-\sigma^*}^{(2)}$, for the interacting two orbitals, σ and σ^* .^{13,16} The σ and σ^* in eq 2 where $H_{\sigma\sigma^*} = \langle \sigma | \hat{H} | \sigma^* \rangle$, $S_{\sigma\sigma^*} = \langle \sigma | \sigma^* \rangle$ and k is a constant, refer to filled and unfilled orbitals, and hence, $\Delta E_{\sigma-\sigma^*}^{(2)}$ includes all types of charge-transfer interactions such as $\pi-\pi^*$, $\text{n}-\pi^*$, $\text{n}-\sigma^*$, etc. The initial attack of the nucleophile (Cl^-) takes place at

$$\Delta E_{\text{CT}} = \Delta E_{\sigma-\sigma^*}^{(2)} = -\sum_{\epsilon_{\sigma^*} - \epsilon_{\sigma}} \frac{2H_{\sigma\sigma^*}^2}{\epsilon_{\sigma^*} - \epsilon_{\sigma}} \cong -\sum \frac{(kS_{\sigma\sigma^*})^2}{\Delta\epsilon} \quad (2)$$

the C_α atom through a HOMO(Cl^-)-LUMO($\text{Y}=\text{CHCl}$) interaction. Thus, the $\text{n}-\pi^*$ ($\text{S}_{\text{N}}\pi$ path) or $\text{n}-\sigma^*$ ($\text{S}_{\text{N}}\sigma$ path) interaction between a lone-pair (n) on the nucleophile (Cl^-) and the π^* LUMO of $\text{Y}=\text{CH}$ or the σ^* LUMO of the C-Cl bond provides a leading term in ΔE_{CT} . However, within the TS, other proximate (geminal and vicinal) $\sigma-\sigma^*$ charge-transfer interactions also contribute to the TS stability.

In all cases the π^* LUMO levels are lower than the σ^* LUMO levels (Table 5), so that the initial attack of the nucleophile (Cl^-) on the π^* orbital ($\text{S}_{\text{N}}\pi$ path) is favored over that on the corresponding σ^* orbital ($\text{S}_{\text{N}}\sigma$ path). Thus, solely on the basis of the energy gap, $\Delta\epsilon$, the $\text{S}_{\text{N}}\pi$ path is predicted to have a better bonding capability¹⁷ and a greater charge-transfer energy than the $\text{S}_{\text{N}}\sigma$ path for all of the reactions. However, this is not true with Y = CH, for which the $\text{S}_{\text{N}}\sigma$ path is energetically preferred to the $\text{S}_{\text{N}}\pi$ path.

The activation energies (at the G2(+)/MP2//MP2/6-311+G** level) for the chloride exchanges in $\text{RY}=\text{CHCl}$ (Y = O, N and CH with R = H) are summarized in Table 6. It is appropriate here to comment on the $\text{S}_{\text{N}}\sigma$ pathway for the chloride exchanges in formyl chloride (Y = O). Characterization of the $\text{S}_{\text{N}}\sigma$ TS (C_{2v}) at four different levels of theory^{5b} (B3LYP/6-311+G**, (16) (a) Klopman, G. *J. Am. Chem. Soc.* **1968**, *90*, 223. (b) Salem, L. *J. Am. Chem. Soc.* **1968**, *90*, 543 and 553. (c) Klopman, G. In *Chemical Reactivity and Reaction Paths*; Klopman, G., Hudson, R. F., Eds.; Wiley: London, 1974; p 55. (d) Fleming I. *Frontier Orbitals and Organic Chemical Reactions*; Wiley: London, 1976; p 27. (e) Klumpp, G. W. *Reactivity in Organic Chemistry*; Wiley: New York, 1982; p 148. (17) Sella, A.; Basch, H.; Hoz, S. *J. Am. Chem. Soc.* **1996**, *118*, 416.

Table 6. Comparison of Activation Energies (ΔE^\ddagger in kcal mol⁻¹) for the Two Reaction Paths, $S_N\sigma$ and $S_N\pi$, in the Chloride Exchanges of $RY=CHCl$ with $R = H$ and $Y = O, N,$ and CH at the G2(+)/MP2//MP2/6-311+G** Level

Y	$\Delta E^\ddagger(\pi)^a$	$\Delta E^\ddagger(\sigma)^a$	$\delta\Delta E^\ddagger(\pi) = \Delta E^\ddagger(\sigma) - \Delta E^\ddagger(\pi)$
O ^b	-9.2	5.9 ^c	+15.1
NH	6.9	14.9	+8.0
CH ₂	28.3	23.0	-5.3

^a Corrected for the zero-point vibrational energy calculated at the MP2/6-311+G** level. ZPEs were scaled by the factor of 0.9748.⁸

^b Reference 5b. ^c Two imaginary frequencies.

Table 7. NBO Lobe (AO) Sizes (in au) at the RHF/6-311+G**//MP2/6-311+G** Level

	σ^*		π^*	
	(C _α)	(C _β)	(C _α)	(Y _β)
CH ₂ =CHCl	0.7448	0.7018	-0.7123	
CH ₃ CH=CHCl	0.7469	0.6816	-0.7317	
HN=CHCl	0.7526	0.7645	-0.6446	
CH ₃ N=CHCl	0.7575	0.7549	-0.6558	
O=CHCl	0.7592	0.8274	-0.5160	

MP2/6-31+G*, MP2/6-311+G**, and QCISD/6-311+G** have all led to two negative eigenvalues in the Hessian matrix, indicating that it is neither a true TS nor an intermediate on the reaction coordinate of the exchange process. Such a TS, a second-order saddle point,⁷ may be considered as a transient structure in the inversion profile of the $S_N\pi$ type TS (C_S), since it has an energy higher by 15.1 kcal mol⁻¹ at the G2(+)/MP2 level^{5b} than the C_S structure and is a maximum with respect to two mutually perpendicular directions.¹⁸

The $S_N\pi$ routes have lower barriers than the $S_N\sigma$ routes for $Y = O$ and N , which reverses to a lower barrier for $S_N\sigma$ than $S_N\pi$ with $Y = CH$, although the barriers for both routes increase in the order $O < N < CH$. These trends are consistent with the progressive elevation of the π^* and σ^* -LUMO levels in the order $O < N < CH$ (Table 5) as the σ -acceptor power decreases. The change in the σ^* level with Y is much smaller than that in the π^* levels, albeit a trend of increase is noticeable. Since the gain in bonding energy is largely controlled by the HOMO-(nucleophile) – LUMO(substrate) energy gap, $\Delta\epsilon$, a greater degree of bonding is expected to be achieved earlier in the reaction in the substrate with lower LUMOs for a given nucleophile (Cl^-), that is, for a given HOMO level. In addition the bonding capabilities also increase with the matrix element, $H_{\sigma\sigma^*}$, the numerator in eq 2, due to the greater second-order stabilization energies gained. In this respect, examination of the lobe (AO coefficient) sizes on the C_α atom may be useful in predicting the reactivity order. Reference to Table 7 reveals that lobe-size changes correctly reflect the relative reactivity as expected from the magnitude of matrix element, which is proportional to the overlap, S in eq 2, between the σ^* and σ (or n) orbital lobes. Interestingly the lobe sizes are greater for the σ^* than π^* orbitals with vinyl (by ~ 0.04 – 0.07), which reverses to the larger π^* lobe with carbonyl chlorides (-0.07), and for the imidoyl chloride the lobe sizes of σ^* and π^* are similar (differs by less than 0.01). This is in line with the preferred reaction pathway found for each compound: $S_N\sigma$ for the vinyl, $S_N\pi$ for the carbonyl and the intermediate between the two for the imidoyl chlorides. The larger lobe size of C_α on σ^* than π^* LUMO for $Y = CH$ is therefore partially responsible for the preferred $S_N\sigma$ pathway with $Y = CH$, despite the *unfavorable energy gap for σ^* relative to π^* interactions*,¹⁹ $\Delta\epsilon(\sigma^*) > \Delta\epsilon(\pi^*)$

(18) Schlegel, H. B. In *Ab Initio Methods in Quantum Chemistry. Part I*; Lawley, K. P., Ed.; Wiley: Chichester, 1987; p 249.

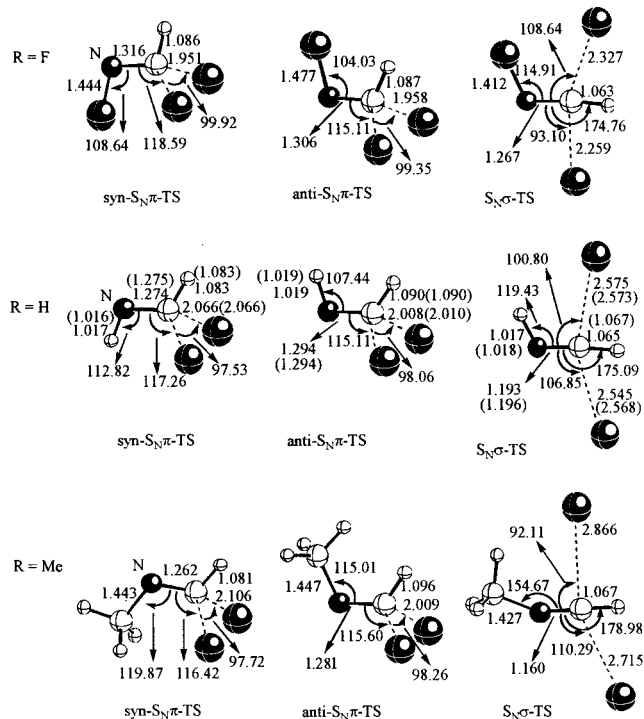


Figure 2. Structures of the adducts in $S_N\pi$ paths, at the MP2/6-311+G** level for $Y = N$ (bond lengths in Å, and angles in degrees). Values in parenthesis are at the QCISD/6-311+G** level.

in eq 2. We also note that the lobe sizes of the π^* and σ^* LUMOs at the C_α atom grow as Y changes from CH to O , which is in line with the general reactivity increase in the same order (Tables 2–4). This is of course a well-known trend of a larger LUMO lobe size of the atom located on the other end of a double bond when a stronger electron acceptor is substituted on the one end of the double bond.^{13a,16d}

Thus, for the nucleophilic substitution reactions of the chloride exchanges, $Cl^- + RY=CHCl \rightleftharpoons RY=CHCl + Cl^-$, the mechanism changes from that of an exclusive $S_N\pi$ to that of an $S_N\sigma$ preferred over an $S_N\pi$ as Y is varied from O (carbonyl) to CH (vinyl), with an intermediate mechanistic behavior for $Y = N$ (imidoyl).

This progressive mechanistic change from $Y = CH$ to O can be explained with the increase in the σ -accepting power and decrease in the π -donating ability of Y from CH to O ²⁰ since electronegativity (χ) of Y increases in the order C ($\chi = 2.55$) $< N$ (3.04) $< O$ (3.41).²¹ The σ -acceptor character of Y is directly related to the electronegativity of Y , which increases steadily across the periodic table from lithium to fluorine, whereas the π -donor ordering is related to the ionization potential of the lone pair of electrons in NH and O , which increases from NH to O , causing the lone pair to be less available for donation.²⁰

Inspection of TS structures in Figures 2 and 3 shows that the π -attack ($S_N\pi$) TSs have relatively tight tetrahedral structure, as we found for the $S_N\pi$ TSs of the carbonyl chlorides.⁵ In contrast, the σ -attack ($S_N\sigma$) TSs are loose with a large degree of $C-Cl$ bond cleavage and small extent of $C-Cl$ bond formation. Bond-length changes (in Tables S3 and S4, Sup-

(19) Lucchini, V.; Modena, G.; Pasquato, L. *J. Am. Chem. Soc.* **1995**, *117*, 2297.

(20) Dill, J. D.; Schleyer, P. v. R.; Pople, J. A. *J. Am. Chem. Soc.* **1976**, *98*, 1663.

(21) McWeeny, R. *Coulson's Valence*, 3rd ed., Oxford University Press: Oxford, 1979; Chapter 6.

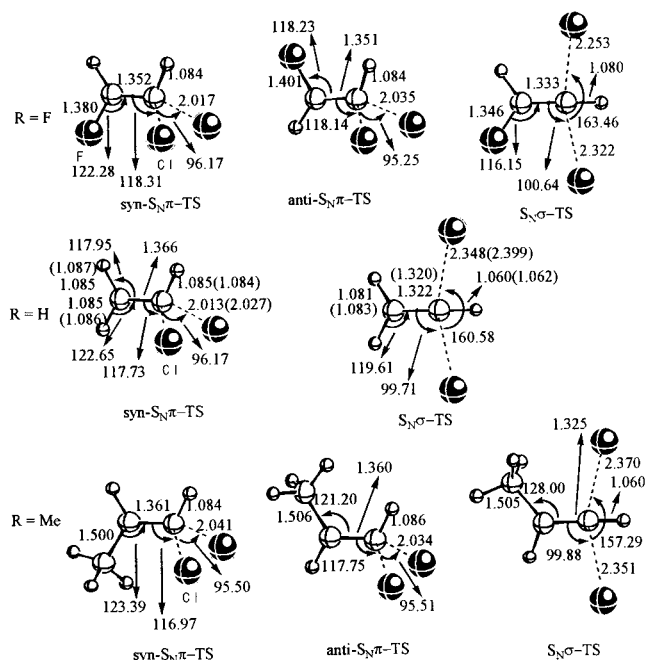


Figure 3. Structures of the adducts in $S_N\pi$ paths, at the MP2/6-311+G** level for $Y = \text{CH}$ (bond lengths in Å, and angles in degrees). Values in parenthesis are at the QCISD/6-311+G** level.

porting Information) and percentage bond-order changes ($\% \Delta n^{5,22}$ in Table S5, Supporting Information) indicate that relatively low degree of bond stretching occurs in the $S_N\pi$ TSs, ~31–47% of C–Cl and 9–22% of C=N and C=C, whereas in the $S_N\sigma$ TSs a large C–Cl bond stretching (~60–90%) and bond contractions of C=N (~8–40%) and C=C (~2%) take place. In other words, the $S_N\pi$ TSs are relatively tight with the two short C–Cl bonds and weakening of C=N and C=C double bonds to those of a single-bond character; conversely the $S_N\sigma$ TSs are relatively loose with the two long C–Cl bonds and strengthening of C=N and C=C double bonds to those of a triple-bond character. In line with these structural changes upon TS formation our natural population analysis (NPA)⁹ (in Tables S6 and S7, Supporting Information) reveals that the double-bond moiety becomes negatively charged in the $S_N\pi$ TSs and positively charged in the $S_N\sigma$ TSs. While the amounts of negative charge developed in the $S_N\pi$ TSs are similar for the imidoyl and vinyl substitutions, the positive charge development in the $S_N\sigma$ TSs is much greater for the imidoyl ($\delta Q = +0.57$ for $R = \text{H}$) than for the vinyl ($\delta Q = +0.27$ for $R = \text{H}$) substitution (Table S8, Supporting Information). Thus, an electron acceptor substituent ($\delta\sigma_R > 0$) should stabilize the $S_N\pi$ -TS by delocalizing the negative charge, whereas an electron donor R ($\delta\sigma_R < 0$) should stabilize the $S_N\sigma$ -TS by delocalizing the positive charge as the energetics in Tables 2–4 show.

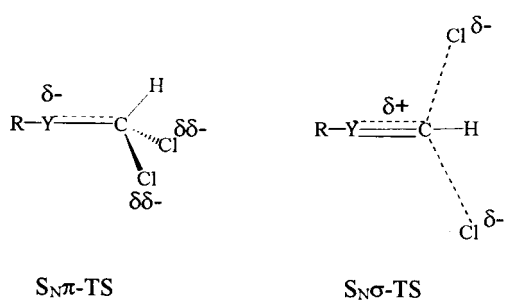
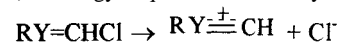


Table 8. MP2/6-311+G** Bond Length (in Å) Changes for the $S_N\sigma$ Paths in the Reactions of $\text{Cl}^- + \text{RY}=\text{CHCl}$ with $Y = \text{O}, \text{N}$, and CH , and $R = \text{H}$

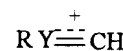
Y	Reactant ^a	TS	RY^+CH		$\Delta E(\text{kcal mol}^{-1})^d$
			Cationic intermediate ^c		
O	O=C	1.191	1.138(72%) ^b	1.120	182.6
	C-Cl	1.765	2.537(67%)	∞	
NH	N=C	1.263	1.193(40%)	1.148	162.1
	C-Cl	1.753	2.575(69%)	∞	
CH_2	C=C	1.335	1.322(11%)	1.235	207.8
	C-Cl	1.729	2.348(59%)	∞	

^a For the syn form. ^b Percentage bond order changes, $\% \Delta n^{5,22}$ in the $S_N\sigma$ -TS. In the limit (100%), $d_{Y=C}$ contracts to that of the cationic intermediate and d_{C-Cl} stretches to ∞ . ^c Acylium (O), nitrilium (N), and vinyl cation (CH). ^d Energy required for heterolytic bond cleavage,



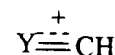
at the MP2/6-311+G** level. Corrected for zero-point vibrational energy (ZPE), and ZPEs were scaled by the factor of 0.9748.⁸

Furthermore, the stability of the $S_N\sigma$ -TS should depend on that of the cationic moiety,

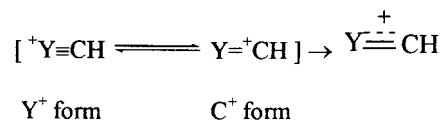


which in turn depends on the σ -accepting power of Y .

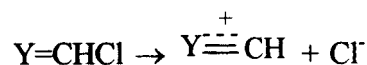
The bond energy gain, ΔBE , upon additional π bond formation from a $Y=C$ double bond to a triple bond, $Y\equiv C$, increases in steps of $\sim 10 \text{ kcal mol}^{-1}$ as Y is changed from C to N and to O : ΔBE 's are $\sim 55, 65$, and 80 kcal mol^{-1} for $C=C \rightarrow C\equiv C$, $N=C \rightarrow N\equiv C$, and $O=C \rightarrow O\equiv C$, respectively.²³ Since an increase in the ionic character of a bond results in a greater stabilization, that is, a stronger bond,²⁴ the successive increase in ΔBE as Y varies from C to O can be ascribed to the increase in the fractional ionic character of the $Y\equiv C$ bond with the increase in the σ -accepting power of Y .²⁴ The polarization of



cation will be stronger as the σ -accepting power of Y increases and the π -donor ability of Y decreases across the periodic table, $\text{CH} \rightarrow \text{N} \rightarrow \text{O}$, rendering stronger C^+ form rather than Y^+ form.



The geometries and energy changes involved in the heterolytic bond cleavage,



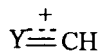
are summarized in Table 8. We note that the formation of the cationic species (acylium (O), nitrilium (N), and vinyl (C)

(22) (a) Houk, K. N.; Gustabson, S. M.; Black, K. *J. Am. Chem. Soc.* **1992**, *114*, 8565. (b) Lee, I.; Kim, C. K.; Lee, B.-S. *J. Comput. Chem.* **1995**, *16*, 1045. (c) Lee, J. K.; Kim, C. K.; Lee, I. *J. Phys. Chem. A* **1997**, *101*, 2893.

(23) Reference 16c, p38.

(24) (a) Reference 18, p153. (b) Reference 13a, Part V.

cations)^{16,25} is the most facile with imidoyl and the least with vinyl. This trend can be explained if we focus upon the $n_Y-\sigma^*_{C-Cl}$ charge-transfer interaction. Since the lone-pair level is higher for N than for O (for Y = CH there is no lone pair), the energy gap, $\Delta\epsilon$, is smaller for N and the $n_N-\sigma^*$ interaction leads to a stronger charge-transfer resulting in a more facile C–Cl bond cleavage than that with $n_O-\sigma^*$ interaction (eq 2). The partial triple bond of

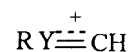


is the shortest with Y = O and the longest with CH in agreement with the relative bond strength of the triple bonds. In the $S_{N\sigma}$ TSs the triple bond formation has progressed to $\sim 70\%$ of that in the cationic species with Y = O but to only 10% with Y = CH and to $\sim 40\%$ with Y = N (Table 8). The positive charge increase in the $S_{N\sigma}$ TS is also larger for Y = N than for CH as noted above. However the progress of bond cleavage for the C–Cl bond in the $S_{N\sigma}$ TSs is similar, 60–70%, for different Y. This is reflected in the similar deformation energies, ΔE_{def} ($\cong 52$ – 58 kcal mol⁻¹ for Y = N and CH with R = H), which are known to represent mainly the bond stretching energies upon TS ($S_{N\sigma}$ TS) formation.²⁶ Naturally deformation energies (**S9**) are somewhat, but not much, higher (by 12–28 kcal mol⁻¹) in the $S_{N\sigma}$ than in the $S_{N\pi}$ TSs since a large degree of endoergic C–Cl bond cleavage is compensated for by a concurrent exoergic triple-bond formation. The energy required to break the C–Cl bond is greatly alleviated by the strong antiperiplanar $n_N-\sigma^*_{C-Cl}$ interaction, which stretches and weakens the C–Cl bond, more in the syn than in the anti substitution. Thus, although the C–Cl bond cleavage occurs to a similar extent, ~ 60 – 70% , the degree of triple bond formation differs depending on Y in the $S_{N\sigma}$ TS. This large difference in the triple bond formation in the TS may also result from the increase in the ionic character (Y = CN < N < O) as the electronegativity of Y increases in the same order.

Since the bond strength of $Y\equiv C$ increases in the order Y = CH < N < O and the extent of triple bond formation in the $S_{N\sigma}$ TS increases in the same order, the $S_{N\sigma}$ reactivity is expected also to increase in that order as we find in Table 6. The activation energy, ΔE^\ddagger , for the $S_{N\sigma}$ path decreases by ~ 10 kcal mol⁻¹ successively from Y = CH to N and to O.

The NBO analysis (**S10**) of the proximate $\sigma-\sigma^*$ charge-transfer interactions, ΔE_{CT} ,⁹ within the TSs shows that the relatively tight $S_{N\pi}$ TSs are stabilized mainly by such charge-transfer interactions. The reactivity of the $S_{N\pi}$ path increases in the same order as that for the $S_{N\sigma}$ path, Y = CH < N < O, but in this case the successive decrease in ΔE^\ddagger is greater, ~ 20 kcal mol⁻¹, as Y is varied. Moreover the absolute proximate $\sigma-\sigma^*$ charge-transfer stabilization energies (Table S10, Supporting Information) are extremely larger in the $S_{N\pi}$ TS ($\Sigma\Delta E^{(2)}_{\sigma-\sigma^*} \cong 800$ and 620 kcal mol⁻¹ for Y = N and CH with R = H, respectively) than in the $S_{N\sigma}$ TS (the corresponding values are ~ 150 kcal mol⁻¹ for both Y = N and CH with R = H). Thus, the increase in the stability of the $S_{N\pi}$ TS from Y = CH to O is much greater, albeit the reactivity order is the same as in the $S_{N\sigma}$ path. As a result, the $S_{N\pi}$ reaction barrier for Y = O is not

only much lower (by $\sim \Delta E^\ddagger = 38$ kcal mol⁻¹) than that for Y = CH, but also lower (by ~ 17 kcal mol⁻¹) than the $S_{N\sigma}$ reaction barrier. This is why the gas-phase chloride exchanges in formyl chloride proceeds exclusively via the $S_{N\pi}$ pathway. However, for the reaction of vinyl chloride, the proximate $\sigma-\sigma^*$ charge-transfer energy in the $S_{N\pi}$ TS is considerably smaller (by ~ 200 kcal mol⁻¹) than that of the imidoyl chloride. This low $\sigma-\sigma^*$ charge-transfer energies for the vinyl chloride in the $S_{N\pi}$ TS are partly due to the absence of a lone-pair, in contrast to the strong $n_Y-\sigma^*_{C-Cl}$ charge-transfer energies involving the lone-pairs on N (imidoyl chloride) and O (formyl chloride). The low charge-transfer energies, ΔE_{CT} , in the $S_{N\pi}$ TS and relatively strong electrostatic interaction (E_{es} is greater by 40–80 kcal mol⁻¹ for $S_{N\sigma}$ than $S_{N\pi}$ TS for Y = CH and N with R = H, Table S8, Supporting Information) in the $S_{N\sigma}$ TS leads to the preference (by ~ 6 kcal mol⁻¹ at the G2(+) level) of the $S_{N\sigma}$ path over the $S_{N\pi}$ for the vinyl chloride.^{3b} The favorable matrix element, $H_{\sigma\sigma^*} \cong kS_{\sigma\sigma^*}$ in eq 2,^{13a} for the vinyl chloride due to a larger AO coefficient, or lobe size, on the C_α atom (greater $S_{\sigma\sigma^*}$ in eq 2) of the σ^* -LUMO than π^* -LUMO should also contribute to the preference of the $S_{N\sigma}$ (vide supra). Thus, the three important factors in favor of the $S_{N\sigma}$ path over the $S_{N\pi}$ path for vinyl chloride are (i) lower charge-transfer stabilization (ΔE_{CT}) due to the absence of lone pair on C (unfavorable for $S_{N\pi}$ path), (ii) stronger stabilization involving the ΔE_{NCT} term (favorable for $S_{N\sigma}$ path), and (iii) the larger lobe size on C_α for the σ^* -LUMO than for the π^* -LUMO (favorable for $S_{N\sigma}$ path). In contrast, for the imidoyl chloride (Y = N) the energetics for both the $S_{N\sigma}$ and $S_{N\pi}$ paths are intermediate between those of formyl and vinyl chloride. In addition, the lobe size on C_α is similar in the σ^* - and π^* -LUMO's (vide supra). As the electron-donating ability of R increases ($\delta\sigma_R < 0$), the stability of the cationic moiety,



in the $S_{N\sigma}$ TS increases but that of the anionic $S_{N\pi}$ TS decreases. This change in the relative stability with a stronger electron donor substituent R makes the $S_{N\sigma}$ TS more stabilized and the $S_{N\pi}$ TS less stable so that the two paths can become comparable as we obtained for the methyl substituted imidoyl chloride.

Experimentally all of the reactions that are reported to proceed by an $S_{N\sigma}$ path with inversion of configuration are known to have such S_{N1} -like TSs⁴ with highly cationic double-bond moiety. Theoretically, in the gas-phase carbonyl substitution, despite the stability of such cationic structure $R-C\equiv O^+$, the extremely stable $S_{N\pi}$ TS leads to the exclusive $S_{N\pi}$ nucleophilic substitution reaction. However, in solution the intervention of an acylium ion intermediate has been at times invoked in the hydrolysis of carbonyl halides,²⁷ which may be reasonable since ionogenic reactions are facilitated in aqueous solution by a strong solvation of the ionic species. In contrast, in the nucleophilic substitution of imidoyl chlorides, the involvement of such an S_{N1} -like TS structure has often been proposed to explain the experimental results of the substitution of halogen by a nucleophile.^{11,28}

Hydrolysis of a series of imidoyl chlorides has been studied kinetically in aqueous solution by Ugi et al.^{28a} The rate is practically independent of steric hindrance effect at the C_α position. In contrast electron-withdrawing substituents at carbon

(25) (a) Radom, L.; Hariharan, P. C.; Pople, J. A.; Schleyer, P. v. R. *J. Am. Chem. Soc.* **1973**, *95*, 6531. (b) Lucchini, V.; Modena, G. In *Applications of MO Theory in Organic Chemistry*; Csizmadia, I. G., Ed.; Elsevier: Amsterdam, 1977; p 268.

(26) (a) Shaik, S. S.; Schlegel, H. B.; Wolfe, S. *Theoretical Aspects of Physical Organic Chemistry. The S_{N2} Mechanism*; Wiley: New York, 1992. (b) Mitchell, D. J.; Schlegel, H. B.; Shaik, S. S.; Wolfe, S. *Can. J. Chem.* **1985**, *63*, 1642.

(27) Williams, A. *Concerted Organic and Bio-organic Mechanisms*; CRC Press: Boca Raton, 2000; p 98 and references therein.

(28) (a) Ugi, I.; Beck, F.; Fetzer, U. *Chem. Ber.* **1962**, *95*, 126. (b) Loeppky, R. N.; Rotman, M. *J. Org. Chem.* **1967**, *32*, 4010.

or nitrogen generally cause a large decrease in reactivity, while electron donors increase the rate of hydrolysis. These observations in solution are in good agreement with our gas-phase theoretical results: the $S_N\sigma$ paths are facilitated by a donor ($R = CH_3$) substituent but are hindered by an acceptor ($R = F$) (Tables 2–4). In a recent theoretical study at the G2(MP2) level, Hammerum et al.,²⁹ have shown that methyl substitution at the imine carbon causes ~ 9.5 – 10.8 kcal mol⁻¹ lowering of the heat of formation, which is greater than that found upon methyl substitution at vinyl but is somewhat less than that observed for carbonyl group, suggesting that the C=N group is less polarized than the carbonyl, C=O, but more polarized than the vinyl, C=C group. The introduction of a methyl group on the nitrogen atom of the imine lowers the heat of formation only by about 1.9 kcal mol⁻¹ suggesting that a larger fraction of the positive charge is located on carbon (C⁺ form) than on N (Y⁺ form) (vide supra).

A two-stage mechanism involving a nitrilium ion pair intermediate has been proposed to account for the results of the kinetic studies.¹¹ Since the ion pair formed in the S_N1 -like processes, that is, a nitrilium cation and a chloride anion, can be stable in the aqueous solution by solvation, the proposed mechanism seems quite reasonable. In view of our present gas-phase theoretical results the mechanism involving such stable nitrilium ion formation in solution is strongly supported.

In summary, the mechanism and reactivity of the gas-phase nucleophilic substitution reactions of the imidoyl carbon are roughly of intermediate nature between those of the carbonyl and vinyl carbon substitutions.

(III) Elimination Reactions. The gas-phase β -elimination of imidoyl chloride with a weak base, Cl⁻, is a relatively facile process with a much lower activation barrier ($\Delta E^\ddagger = -10.6$ and -12.6 kcal mol⁻¹ at the G2(+) level for syn and anti elimination, respectively) than substitution ($\Delta E^\ddagger = 7.1$ kcal mol⁻¹, Table 4). The barrier heights are much lower than the corresponding β -elimination barrier ($\Delta E^\ddagger = 22.0$ kcal mol⁻¹ at

the G2(+)(MP2) level) for the vinyl chloride.^{3b} This can be ascribed to the higher acidity of the β -proton³⁰ and more facile C–Cl bond cleavage due to the $n_N-\sigma^*_{C-Cl}$ charge-transfer interaction in the imidoyl chloride than in vinyl chloride. The latter effect seems to be greater since the percentage bond order change in the TS (Table S11, Supporting Information) is greater for the stretching of the C–Cl bond ($\sim 40\%$) than for the N–H bond ($\sim 30\%$). Thus, the eliminations are of E2 type as we found for the β -elimination in the vinyl chloride,^{3b} for which, however, the TS is reached at a somewhat later stage ($\sim 60\%$ C–H and C–Cl bond stretching in the TS) along the reaction coordinate. Thus, the earlier TS for the β -elimination of imidoyl than vinyl chloride is in accord with the Bell–Evans–Polanyi (BEP) principle,³¹ which asserts that the earlier the TS along the reaction coordinate, the lower is the activation barrier. In almost all of the actual reactions in solution, however, the unsubstituted azomethines, for example, HN=CHCl, are rarely used, but the RN=CR'Cl type, disubstituted imidoyl compounds are involved.^{11,32} Therefore, the extremely facile β -elimination reactions are not observed and are not important in practice. The substitution reactions provide the major reaction pathway.

Acknowledgment. We thank Inha University and the Ministry of Education, Brain Korea 21 Project for support of this work.

Supporting Information Available: Figure showing structures of reactants for Y = CH and additional tables (PDF). This material is available free of charge via the Internet at <http://pubs.acs.org>.

JA0033584

(30) Hopkinson, A. C. In *Applications of MO Theory in Organic Chemistry*; Csizmadia, I. G., Ed.; Elsevier: Amsterdam, 1977; p 194.

(31) Pross, A. *Theoretical and Physical Principles of Organic Reactivity*; Wiley: New York, 1995; p 139.

(32) Morath, R. J.; Stacy, G. W. In *The Chemistry of the Carbon-Nitrogen Bond*; Patai, S., Ed.; Interscience, New York, 1970; Chapter 8.

(29) Hammerum, S.; Solling, T. I. *J. Am. Chem. Soc.* **1999**, *121*, 6002.